to the value in the nonmagnetic isostructural compound ThP. T_2' is determined by homogeneous internuclear dipolar interactions.

(v) The spin-lattice relaxation time of ^{31}P in the paramagnetic state of the $UP_{1-x}S_x$ system is three orders of magnitude shorter than T_1 in ThP, does not have the simple temperature dependence that occurs in metals ($T_1T=$const), and *increases* with temperature for all compositions, regardless of the magnetic ordering. The product T_1T *strongly increases* with temperature for all compositions, thus contradicting the previously proposed theory of Silbernagel *et al.*[9] The present results support the treatment given recently by Fradin.[11] For the ferromagnetic compositions a relation $T_1TK=$const is obtained, similar to Fradin's result[11] in PuP and also to the result in β-UH_3,[7] although the latter involves larger experimental errors. For the antiferromagnetic compositions a different relation is obtained, but it cannot be formulated in a simple formula as in the case of ferromagnetic compositions. Relations such as $T_1TK^2=$const or $T_1T=D(T-\theta_1)$ can be used to approximately characterize the temperature behavior of T_1 in the antiferromagnetic compositions, with the latter [Eq. (14)] having some basis in the treatment of Fradin.[11]

The NMR results of ^{31}P in the paramagnetic state of the $UP_{1-x}S_x$ system make use of the special magnetic properties of this system. The extension of the NMR work to the ordered state would provide a direct relationship with the magnetization and neutron diffraction studies of the $UP_{1-x}S_x$ system.

ACKNOWLEDGMENTS

We wish to thank D. O. Van Ostenburg for his interest in this study, his encouragement in all phases of this research, and his review of the manuscript. Thanks are also due to J. J. Spokas for his comments on the manuscript and to F. Y. Fradin for providing his paper prior to publication and for helpful comments. We also wish to thank S. D. Smith for assistance in the sample preparation.

PHYSICAL REVIEW VOLUME 187, NUMBER 2 10 NOVEMBER 1969

Mössbauer Study of Several Ferrimagnetic Spinels*

G. A. SAWATZKY†, F. VAN DER WOUDE,†‡ AND A. H. MORRISH
Department of Physics, University of Manitoba, Winnipeg 19, Canada

(Received 26 May 1969)

The ferrimagnetic spinels Fe_3O_4, $NiFe_2O_4$, $CoFe_2O_4$, $MnFe_2O_4$, and $MgFe_2O_4$ have been prepared and studied with the Mössbauer-effect technique over a wide temperature range both with and without large applied magnetic fields. The cation distributions have been determined and compared with magnetization measurements. For $CoFe_2O_4$ and $MgFe_2O_4$, this distribution depends on the heat treatment; two extremes—quenched and slowly cooled samples—have been investigated. The hyperfine magnetic fields at Fe^{57} nuclei in *A* and *B* sites have been obtained as a function of temperature. A number of hyperfine fields are identified with the *B* sites of $CoFe_2O_4$, $MnFe_2O_4$, and $MgFe_2O_4$ and attributed to the kind and distributions of cations in the nearest-neighbor *A* sites. From the data, the ratio of the Co(*A*)-Fe(*B*) and Mn(*A*)-Fe(*B*) to the Fe(*A*)-Fe(*B*) superexchange interactions is found to be 0.68 and 0.66, respectively. Since the Mössbauer spectra provides no evidence for Fe^{2+} ions in $MnFe_2O_4$, a canted spin arrangement for the Mn ions in *A* and *B* sites is proposed to account for the small observed magnetization.

I. INTRODUCTION

A FERRIMAGNETIC spinel can be represented by the formula (M)[M_2']O_4, in which the round and square brackets refer to metal ions situated in an oxygen tetrahedron or octahedron, respectively. If the tetrahedral (*A*) and octahedral (*B*) sites are occupied by metal ions possessing a magnetic dipole moment, cooperative phenomena known as ferrimagnetism may be observed below a particular temperature. The properties of these materials depend on what kinds of metal ions are present in the different sites and how these are distributed. Spinels with only divalent ions in tetrahedral or in octahedral sites are called "normal" or "inverse," respectively. The main cause for a cooperative behavior of the magnetic dipoles in a spinel is the antiferromagnetic *A-B* superexchange interaction.

Ferrimagnetism was discovered in materials with a spinel structure. Consequently, these materials have been investigated very often.[1-3] Also the Mössbauer-effect (ME) technique has been used to investigate

---

* Supported by the National Research Council of Canada.

† Present address: Solid State Physics Laboratory, University of Groningen, Groningen, The Netherlands.

‡ Member of the staff of the Foundation for Fundamental Research of Matter (F.O.M.) of The Netherlands.

[1] E. W. Gorter, Philips Res. Rept. 9, 1 (1954).

[2] G. Blasse, Philips Res. Rept. Suppl. 3, 1 (1964).

[3] J. Smit and H. P. J. Wijn, *Ferrites* (John Wiley & Sons, Inc., New York, 1959).

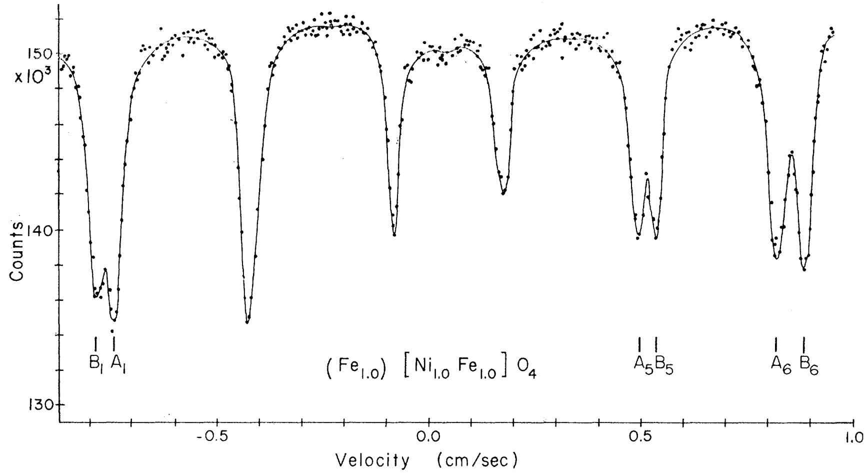

FIG. 1. Mössbauer spectrum of $NiFe_2O_4$ at room temperature. *A* and *B* refer to Fe^{57} in *A* and *B* sites.

these materials. The interpretation of data on spinels with only di- and trivalent ions varies considerably. Even the very simple case of the completely inverse spinel $NiFe_2O_4$ has found different interpretations.[4,5] The difficulties are partly due to the broadened lines.

In this paper we present our results on Fe_3O_4, $CoFe_2O_4$, $NiFe_2O_4$, $MnFe_2O_4$, and $MgFe_2O_4$. The results on Fe_3O_4 have been published already[6] and will only be summarized here. Some of the results on the not completely inverse $CoFe_2O_4$ have also been reported on.[7] Now we will pay more attention to the temperature-dependent broadening of the absorption lines ascribed to *B*-site iron nuclei and show how from these widths information concerning superexchange strengths can be obtained. The various explanations for the low magnetic moment of $MnFe_2O_4$ will be tested.

In Sec. II we describe the experimental setup and preparation of the investigated materials. The experimental results on Fe_3O_4 are summarized in Sec. III. The data of the other ferrites are presented and discussed in Sec. IV. A calculation of the superexchange strengths is given in Sec. V.

II. EXPERIMENTAL

The materials were prepared by the following techniques: mixing of the separate oxides, co-precipitation of the hydroxides, or formation of the oxalate. All of these methods require subsequent heat treatments. $NiFe_2O_4$ was prepared by both the oxalate method and the hydroxide method. The material was then heated at a relatively low temperature to form the oxides. After this step, the sample was prefired at 900°C for 24 h and then sintered at 1250°C for 24 h. The magnetic moment and Mössbauer spectra of the materials prepared in these two ways did not show any difference. $CoFe_2O_4$ was prepared in all three ways. For the hydroxide and oxalate methods the heat treatment was the same as that described for $NiFe_2O_4$. For the heat treatment after the thorough mixing of the oxides, the material was prefired twice at 900°C for 24 h, next ground, and finally sintered at 1250–1400°C for 24 h.

$MgFe_2O_4$ and $MnFe_2O_4$ were prepared by the oxide method with the same heat treatment described earlier for $CoFe_2O_4$.

The final materials were subjected to two different heat treatments. The quenched (q) materials were obtained by heating the sample at 1250–1400°C and water quenching to room temperature. The slowly cooled (s.c.) materials were obtained by furnace cooling from 1250°C at a rate of 4°C/h. The $MgFe_2O_4$ (s.c.) was then heated at 350°C for 24 h. The $MnFe_2O_4$ (s.c.) had decomposed to the separate oxides, as could easily be seen from x-ray spectra and the Mössbauer spectrum.

Magnetic moment measurements were carried out with a vibrating sample magnetometer. These measurements were made at 296, 77, and 4.2°K in fields up to 18 kOe.

ME experiments were done either with a constant-velocity drive, or with a constant-acceleration drive using a 1024 multichannel analyzer. The furnace used has been described elsewhere.[6] The liquid-nitrogen cryostat was similar in design to that described by Sharon and Treves,[8] except that we used a cold finger instead of a flow-through system.

III. Fe_3O_4

Fe_3O_4 has been important for our study on the ferrimagnetic spinels. The relation between temperature dependence of the hyperfine magnetic field at Fe^{57} nuclei and the corresponding sublattice magnetization for *A* and *B* sites, respectively, has been determined experimentally.[6] Also the relation between the area

---

[4] D. Kedem and T. Rotham, Phys. Rev. Letters **18**, 165 (1967).

[5] J. Chappert and R. B. Frankel, Phys. Rev. Letters **19**, 570 (1967).

[6] F. van der Woude, G. A. Sawatzky, and A. H. Morrish, Phys. Rev. **167**, 533 (1968).

[7] G. A. Sawatzky, F. van der Woude, and A. H. Morrish, J. Appl. Phys. **39**, 1204 (1968).

[8] B. Sharon and D. Treves, Rev. Sci. Instr. **37**, 1252 (1966).

ratio of peaks assigned to Fe^{57} ions in B and A sites and the ratio of occupation numbers in B and A sites could be established.[9] Since we will apply these results, we now summarize them. (1) The shapes of the H_{hpf} versus T curve and the M versus T curve are the same within the experimental accuracy of 1% over a 500°K temperature interval. (2) The ratio of the recoilless fractions for the two sites f_B'/f_A' is equal to 0.94 ± 0.02 at room temperature. This means that the ratio of the areas of the B peaks to the A peaks is 6% lower than the ratio of the corresponding occupation numbers.

Because of the similarity in many properties of the ferrites Fe_3O_4, $NiFe_2O_4$, $CoFe_2O_4$, $MnFe_2O_4$, and $MgFe_2O_4$, it seems reasonable to make use of the results mentioned above for the other ferrites as well.

IV. EXPERIMENTAL RESULTS

A. $NiFe_2O_4$

The Mössbauer spectrum of $NiFe_2O_4$ shown in Fig. 1 is easily interpreted as being due to two six-line hyperfine patterns corresponding to Fe^{57} in B and A sites. The assignments of the peaks to Fe^{57} in A and B sites as shown in Fig. 1 is simply verified by recording spectra in an applied magnetic field. For the ferrimagnetic spinels, the applied field will add to the hyperfine field at A-site nuclei and subtract from the hyperfine field at B-site nuclei. It has been suggested by Kedem and Rothem[4] that $NiFe_2O_4$ has a Yafet-Kittel[10] type of spin arrangement. Chappert and Frankel,[5] however, have shown that the spin arrangement in $NiFe_2O_4$ is of the Néel collinear type. This agrees with the ferromagnetic Ni(B)-Fe(B) interaction suggested by Morel[11] and also with the very small antiferromagnetic Fe(B)-Fe(B) interaction indicated by the low Néel temperature found for $ZnFe_2O_4$ and $CdFe_2O_4$.[12]

It has generally been assumed that $NiFe_2O_4$ is an inverse spinel. This can be verified by measuring the area ratio I_B/I_A of the Mössbauer patterns corresponding to Fe^{57} in B and A sites. This area ratio was found to be 1.02 ± 0.06 for line 1 of a spectrum taken at 106°K. At this temperature the correction required for the ratio of recoilless fractions[9] is negligible. This area ratio confirms that $NiFe_2O_4$ is an inverse spinel.

The magnetic moment measured at 4.2°K was found to be $2.20\mu_B$ per unit chemical formula, which implies a moment of $2.20\mu_B$ per Ni^{2+} ion, since the Ni ions are almost solely located in the B sites.

Measurements of the temperature dependence of the hyperfine field at Fe^{57} nuclei in A and B sites yielded results in agreement with those reported by Morel.[11] These results show, as expected, that the B-site hyperfine field decreases more rapidly with increasing temperature than the hyperfine field at A-site Fe^{57} nuclei. The ferrimagnetic Néel temperature (T_{FN}) was found to be 868°K by the thermal scanning technique.[6]

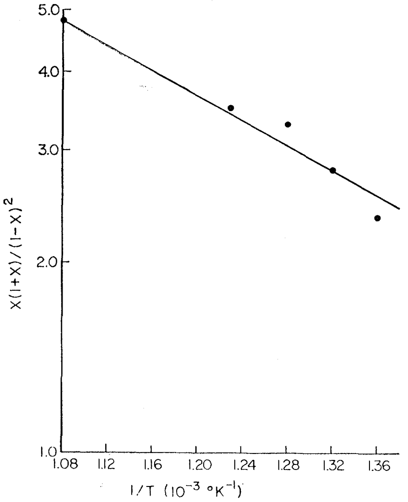

FIG. 2. Plot on a semilog scale of $x(1+x)/(1-x)^2$ versus $1/T$, where T is the temperature at which the material was heated. x is the concentration of Co^{2+} ions in the A sites calculated from the magnetic moment of the material.

It should be noted that both the A- and B-site absorption lines are reasonably narrow in $NiFe_2O_4$ and show no apparent structure. Also at higher temperatures there is only little broadening. This is in contrast to the spectra of $CoFe_2O_4$, $MnFe_2O_4$, and $MgFe_2O_4$ which will be discussed later.

B. $CoFe_2O_4$

The results obtained for $CoFe_2O_4$ have already been presented in part elsewhere.[7] One of the results reported was that $CoFe_2O_4$ was not completely inverse and that the degree of inversion depended on the heat treatment. The cation distribution found together with the magnetic moment measurements implied that the magnetic moment of a Co^{2+} ion in an octahedral site was considerably lower than the usually accepted value of $3.5\mu_B$.[13,14] The magnetic moment was, however, measured at 77°K. We have now extended this measurement to 4.2°K and have extrapolated the values to infinite internal field. We find a magnetic moment of $(3.45\pm0.05)\mu_B$ for $CoFe_2O_4$ (s.c.) and $(4.00\pm0.05)\mu_B$ for $CoFe_2O_4$ (q).

The cation distribution reported previously[7] for these two materials was not corrected for a possible difference in the recoilless fractions of Fe^{57} in A and B sites. By using the corrections found for Fe_3O_4,[6] the

---

[9] G. A. Sawatzky, F. van der Woude, and A. H. Morrish, Phys. Rev. **183**, 383 (1969).

[10] Y. Yafet and C. Kittel, Phys. Rev. **87**, 290 (1952).

[11] J. P. Morel, J. Phys. Chem. Solids **28**, 629 (1967).

[12] J. Sawicki, Czech. J. Phys. **B17**, 371 (1967).

[13] J. L. Slonczewski, Phys. Rev. **110**, 1341 (1958).

[14] M. Tachiki, Progr. Theoret. Phys. (Kyoto) **23**, 1055 (1960).

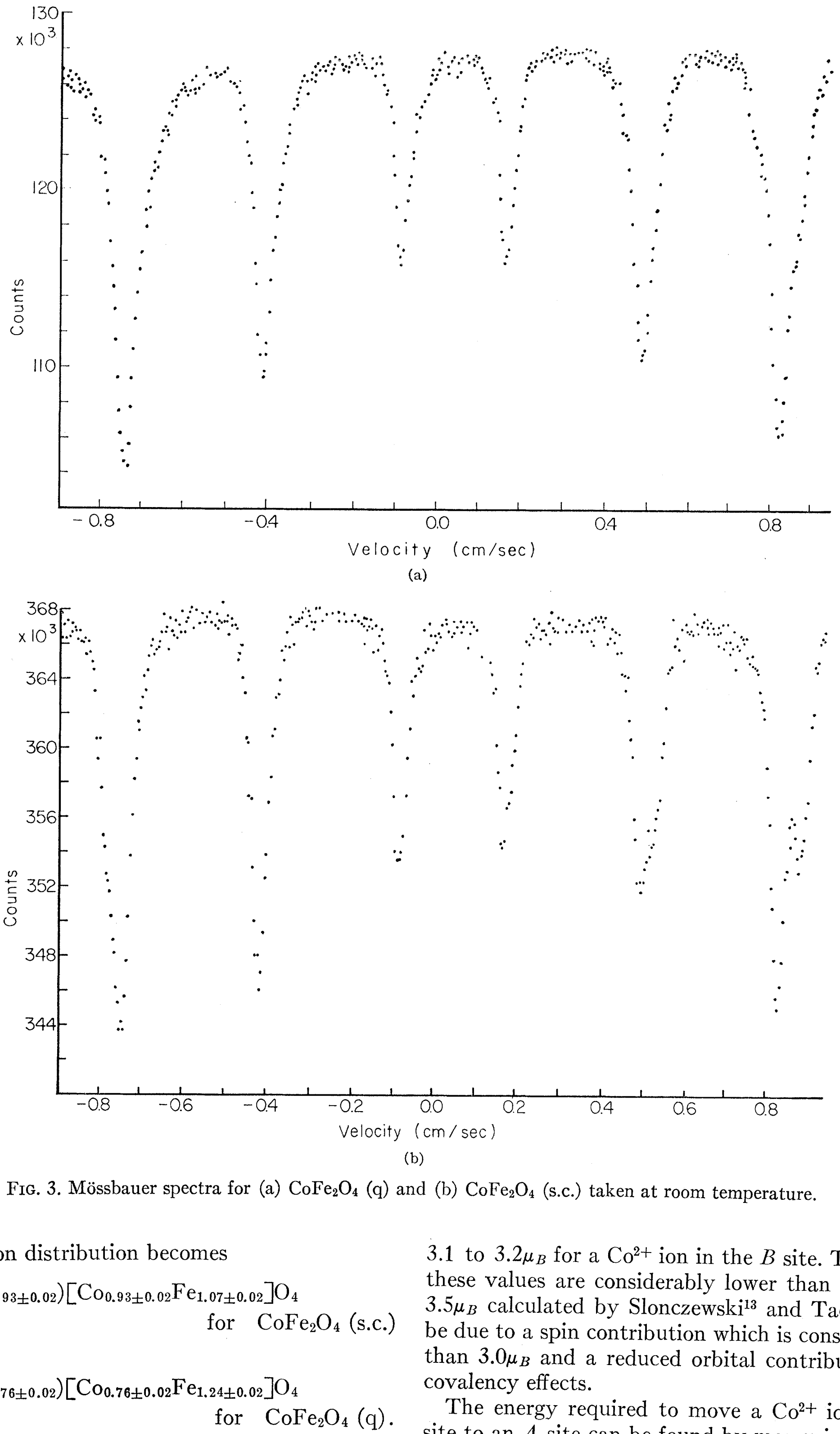

FIG. 3. Mössbauer spectra for (a) $CoFe_2O_4$ (q) and (b) $CoFe_2O_4$ (s.c.) taken at room temperature.

corrected cation distribution becomes

$$(Co_{0.07\pm0.02}Fe_{0.93\pm0.02})[Co_{0.93\pm0.02}Fe_{1.07\pm0.02}]O_4 \quad \text{for} \quad CoFe_2O_4 \text{ (s.c.)}$$

and

$$(Co_{0.24\pm0.02}Fe_{0.76\pm0.02})[Co_{0.76\pm0.02}Fe_{1.24\pm0.02}]O_4 \quad \text{for} \quad CoFe_2O_4 \text{ (q)}.$$

By assuming that Co^{2+} in an A site has a magnetic moment of $3.0\mu_B$, we then get a magnetic moment of 3.1 to $3.2\mu_B$ for a Co^{2+} ion in the B site. The fact that these values are considerably lower than the value of $3.5\mu_B$ calculated by Slonczewski[13] and Tachiki[14] could be due to a spin contribution which is considerably less than $3.0\mu_B$ and a reduced orbital contribution due to covalency effects.

The energy required to move a Co^{2+} ion from a B site to an A site can be found by measuring the cation distribution as a function of the heat treatment. In Fig. 2 we show a plot of $\ln[x(1+x)/(1-x)^2]$ versus

$1/T$, where x is the A-site Co concentration found from the magnetic moment of $CoFe_2O_4$ measured at room temperature. The straight line drawn has a slope corresponding to an energy of 0.19 eV which is slightly higher than the value of 0.14 eV found for $CuFe_2O_4$ and $MgFe_2O_4$.[15–17] It should be pointed out that calculations of the B-site stabilization[2,18,19] are consistent with our result that $CoFe_2O_4$ is not completely inverse.

The broadening of the B-site lines of the Mössbauer spectra was interpreted as being due to a distribution in hyperfine fields caused by the distribution of Co and Fe nearest A-site neighbors.[7] This interpretation will now be discussed in greater detail.

The assumption is that the hyperfine magnetic fields at B-site Fe^{57} nuclei are a function of the occupation of the six nearest A sites by Fe^{3+} and Co^{2+} ions. Then the intensity ratio of the different B-site peaks can be calculated since it is proportional to the ratio of the probabilities of the different surroundings. So we have

$$I(n)=\binom{6}{n}(1-c)^{6-n}c^{n}, \qquad (1)$$

where $I(n)$ is the relative intensity of the B peak with n Fe^{3+} ions in the nearest-neighbor A sites and c is the concentration of Fe^{3+} ions in A sites. For an inverse spinel, c equals 1; and for a normal spinel, c equals 0. The calculated relative intensities of the B sites in slowly cooled $CoFe_2O_4$ with $c=0.93$ are $I(6):I(5):I(4):I(3)::0.65:0.29:0.05:0.00$, and for quenched $CoFe_2O_4$ with $c=0.76$ they are $I(6):I(5):I(4):I(3)::0.19:0.37:0.29:0.12$.

In Figs. 3(a) and 3(b), the room-temperature spectra of $CoFe_2O_4$ (q) and $CoFe_2O_4$ (s.c.), respectively, are shown. The spectrum of $CoFe_2O_4$ (s.c.) differs from that of $NiFe_2O_4$ shown in Fig. 1. The sixth B-site line seems to be less intense than the A-site line if we identify them in the same way as was done for $NiFe_2O_4$. However the spectrum in an applied field of 55 kOe[7] showed that the B-site area was larger than that corresponding to Fe^{57} in A sites. This means that there must be a large distribution of B-site hyperfine fields and that the hyperfine field for some of the Fe^{57} in B sites must be nearly the same as that for Fe^{57} in A sites. The spectrum of $CoFe_2O_4$ (q) shows the same feature, but the distribution in B-site hyperfine fields must be even larger.

TABLE I. Mössbauer data on $CoFe_2O_4$.

	A	$B1$	$B2$	$B3$	$B4$
H_{hpf} (kOe)	490	515	499	475	445
Isomer shift[a] (mm/sec)	0.45	0.48	0.58	0.55	0.58

[a] Relative to Fe^{57} in a Cr matrix; error in $H_{\mathrm{hpf}}=\pm5$ kOe, error in $IS=\pm0.04$ mm/sec.

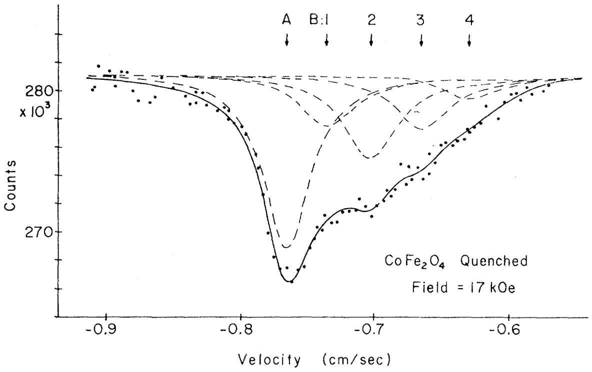

FIG. 4. Line 1 of the Mössbauer spectrum of $CoFe_2O_4$ (q) in an applied field of 17 KOe. A and B refer to Fe^{57} in A and B sites, respectively. B:1, 2, 3, 4 refer to Fe^{57} in B sites with 0, 1, 2, 3 nearest-neighbor Co A-site ions, respectively.

In Fig. 4 is shown line 1 of a spectrum of $CoFe_2O_4$ (q) in an applied field of 17 kOe at room temperature. Also shown is the fit obtained to the sum of five Lorentians, one for Fe^{57} in A sites and four for Fe^{57} in B sites. The fit was done by imposing constraints on the B-site intensities such that the intensities were proportional to the probabilities that an Fe B-site ion has 6 Fe, 5 Fe 1 Co, 4 Fe 2 Co, and 3 Fe 3 Co nearest-neighbor A-site ions. It is seen that the spectrum can be fitted in good detail by assuming such a model. Line 6 of the spectrum is very similar to line 1. The hyperfine fields and isomer shifts obtained from the fit are listed in Table I. The important property is that the hyperfine field at the Fe^{57} B-site nucleus decreases with an increase in the number of Co A-site nearest neighbors.

From Mössbauer spectra collected at various temperatures between 100 and 550°K we concluded that the range in B-site hyperfine fields increases with increasing temperature. This deduction is obvious by inspection because the broadening of the B-site lines is very dependent on temperature and because structure in the B-site lines appears at elevated temperatures.

The hyperfine fields at various temperatures for $CoFe_2O_4$ (s.c.) and $CoFe_2O_4$ (q) have been shown in Fig. 2 of Ref. 7. It can be seen that the hyperfine field at the Fe^{57} B-site nucleus decreases more rapidly with increasing temperature as the number of Co^{2+} A-site nearest neighbors increases. This is consistent with the Co(A)-Fe(B) superexchange interaction being less than the Fe(A)-Fe(B) interaction. A calculation of the various superexchange interactions is given in Sec. V.

Another interesting property is that the hyperfine field at Fe^{57} B-site nuclei at 0°K decreases with an increasing number of Co A-site nearest neighbors. This hyperfine field seems to decrease by 6–10 kOe for each Fe A-site nearest neighbor replaced by a Co ion. This property will be discussed in a subsequent

---

[15] F. Bertaut, J. Phys. Radium **12**, 252 (1951).

[16] L. Néel, Compt. Rend. **230**, 190 (1950).

[17] R. Pauthenet, Compt. Rend. **230**, 1842 (1950).

[18] D. S. McClure, J. Phys. Chem. Solids **3**, 311 (1957).

[19] J. D. Dunitz and L. E. Orgel, J. Phys. Chem. Solids **3**, 318 (1957).

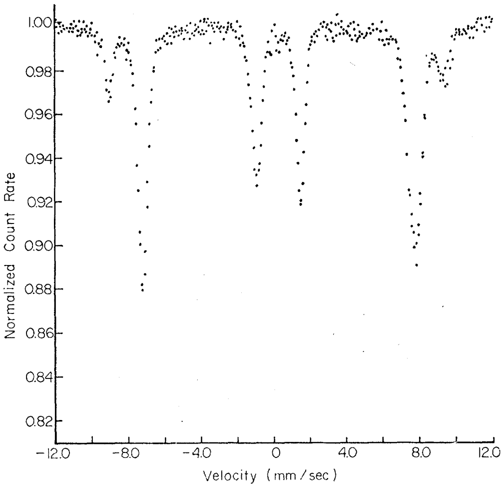

FIG. 5. Mössbauer spectrum of $MnFe_2O_4$ in an applied field of 55 KOe at 7°K.

paper on supertransferred hyperfine interactions and covalency.[20]

C. $MnFe_2O_4$

It has been shown from neutron diffraction and ME measurements[21,22] that $MnFe_2O_4$ has the cation distribution given by $(Mn_{0.8}Fe_{0.2})[Mn_{0.2}Fe_{1.8}]O_4$. Hence this material is suitable for a Mössbauer study of the kind just described for $CoFe_2O_4$. $MnFe_2O_4$ shows another property which has drawn much attention, viz., its low magnetic moment. The magnetic moment per unit chemical formula for the case where all the Mn ions are divalent is expected to be $5\mu_B$ at 0°K. The measured magnetic moments, however, range from $4.5\mu_B$ to $4.8\mu_B$.[17,21,23] These low values may be due to several causes: For example, some of the Mn ions could be trivalent and some of the Fe ions could be divalent.[24,25] However, calculations by Lotgering[26] have shown that this possibility is unlikely. Since Mössbauer spectra of Fe^{2+} and Fe^{3+} ions are usually distinguishable, the Mössbauer effect could provide a means for determining whether or not there is any Fe^{2+} present.

For this reason, we have collected a Mössbauer spectrum of $MnFe_2O_4$ at 7°K in an applied field of 55 kOe with the field direction parallel to the direction of propagation of the γ rays. Although in Fe_3O_4 at temperatures below the Verwey transition the Fe^{2+} spectrum is not well resolved from the B- and A-site Fe^{3+} spectra, Evans *et al.*[27] have shown that in an applied field the Fe^{2+} spectrum is at least partially resolved. However, Fe_3O_4 may be a more complicated example because of the presence of two Fe^{2+} spectra which are probably due to the twinning below the transition temperature.[28] The reason for taking the $MnFe_2O_4$ spectrum at such a low temperature is to reduce the probability for electron hopping and hence permit resolution of the Fe^{2+} and Fe^{3+} spectra. The spectrum shown in Fig. 5 shows no evidence of any component in addition to the Fe^{3+} A- and B-site spectra. This suggests that there is little if any Fe^{2+} in the B sites of $MnFe_2O_4$, in agreement with Lotgering's calculation.[26]

Another possible explanation for the low magnetic moment could be that the spin arrangement is not collinear. If, however, we assume that the Fe(B) spins are canted as in the Yafet-Kittel[10] triangular spin arrangement or in a random manner as suggested by Geller,[29] we would require an average angle between the B-site spin and the magnetization direction of about $\theta = \cos^{-1} 0.95$. In the Mössbauer spectrum in the 55-kOe field (Fig. 5) we should see a $\Delta m = 0$ transition with intensity about 0.06 of the $\Delta m = 1$, $\frac{3}{2} \rightarrow \frac{1}{2}$ B-site line, i.e., the intensity would be about 0.54 of the A-site line. From the spectrum in the 55-kOe field we can see that the upper limit of the intensity in the $\Delta m = 0$ region is 0.1 of the $\Delta m = 1$, $\frac{3}{2} \rightarrow \frac{1}{2}$ A-site line. This shows that if there is a noncollinear spin arrangement the Fe ions are not involved to a large enough extent to explain the low magnetic moment.

In the case of $MnFe_2O_4$ there is, however, another possibility. As will be shown later, the Mn(A)-Fe(B) interaction is about 0.66 of the Fe(A)-Fe(B) interaction. We expect the Mn(A)-Mn(B) superexchange interaction to be even smaller because of the low Néel temperature of Mn_3O_4. Since, however, the B-site neighbors of an Mn ion in the B sites are mostly Fe neighbors, the Mn(B)-Fe(B) superexchange interaction might be comparable to the Mn(B)-Mn(A) interaction. The spin

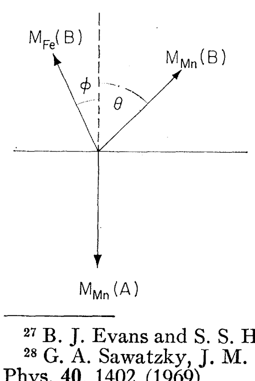

FIG. 6. Postulated spin arrangement in $MnFe_2O_4$, $M_{Fe}(B)$, $M_{Mn}(B)$ and $M_{Mn}(A)$ refer to the magnetic moments of Fe and Mn in B and A sites.

---

[20] F. van der Woude, G. A. Sawatzky, and A. H. Morrish, (to be published).

[21] J. H. Hastings and L. M. Corliss, Phys. Rev. **104**, 328 (1961).

[22] G. A. Sawatzky, F. van der Woude, and A. H. Morrish, Phys. Letters **25A**, 147 (1967).

[23] G. Guillaud, J. Phys. Radium **12**, 239 (1951).

[24] L. G. van Uitert, J. Chem. Phys. **23**, 1883 (1955).

[25] F. W. Harrison, W. P. Osmond, and R. W. Teale, Phys. Rev. **106**, 865 (1957).

[26] F. K. Lotgering, J. Phys. Chem. Solids **25**, 95 (1964).

[27] B. J. Evans and S. S. Hafner, J. Appl. Phys. **40**, 1411 (1969).

[28] G. A. Sawatzky, J. M. D. Coey, and A. H. Morrish, J. Appl. Phys. **40**, 1402 (1969).

[29] S. Geller, H. J. Williams, G. P. Espinosa, and R. C. Sherwood, Bell System Tech. J. **43**, 565 (1964).

arrangement in this situation might be as shown in Fig. 6. The magnetic moments $M_{\mathrm{Mn}}(B)$ at Mn(B) ions could make a fairly larger angle θ with $M_{\mathrm{Mn}}(A)$ whereas the angle ϕ between $M_{\mathrm{Fe}}(B)$ and $M_{\mathrm{Mn}}(A)$ could be very small.

With the following assumptions and approximations we can show that such a spin arrangement is energetically possible. (1). The Fe(B)-Fe(B) interaction can be neglected in comparison with the Fe(B)-Mn(A) interaction. This means that all the Fe(B) moments will be parallel. (2). The Mn(B)-Mn(B) interaction can be neglected in comparison with the Mn(A)-Mn(B) interaction. This means that the Mn(B) moments will all make the same angle θ with the magnetic moment of the A-site ions. (3). For simplicity we assume all the A-site ions to be identical. The calculations can easily be extended to the more general case.

The molecular field acting on the various spins will be given by

$$\mathbf{H}(\mathrm{Mn}(B))=N_{AB}'\mathbf{M}_A+N_{BB}\mathbf{M}_B\,,$$
$$\mathbf{H}(\mathrm{Fe}(B))=N_{AB}\mathbf{M}_A+N_{BB}\mathbf{M}_B'\,,$$
$$\mathbf{H}(\mathrm{Mn}(A))=N_{AB}'\mathbf{M}_B'+N_{AB}\mathbf{M}_B\,,$$

where N_{AB}' is the Mn(A)-Mn(B) molecular-field coefficient, N_{AB} is the Fe(B)-Mn(A) molecular-field coefficient, and N_{BB} is the Mn(B)-Fe(B) molecular field coefficient; all molecular field coefficients are taken to be positive. $\mathbf{M}_A$,$\mathbf{M}_B$, and $\mathbf{M}_B'$ are the magnetic moments of the Mn(A), Fe(B), and Mn(B) ions, respectively. The free energy is written as

$$\begin{aligned}E&=-\sum_i \mathbf{H}_i\cdot\mathbf{M}_i\\&=2N_{AB}'|\mathbf{M}_A||\mathbf{M}_B'|\cos\theta-2N_{BB}|\mathbf{M}_B||\mathbf{M}_B'|\cos(\theta+\phi)\\&\qquad+2N_{AB}|\mathbf{M}_A||\mathbf{M}_B|\cos\phi.\end{aligned}$$

On minimizing this energy with respect to θ and ϕ we get

$$+N_{AB}'|\mathbf{M}_A||\mathbf{M}_B'|\sin\theta-N_{BB}|\mathbf{M}_B||\mathbf{M}_B'|\sin(\theta+\phi)=0 \quad (2)$$

and

$$-N_{BB}|\mathbf{M}_B||\mathbf{M}_B'|\sin(\theta+\phi)+N_{AB}|\mathbf{M}_A||\mathbf{M}_B|\sin\phi=0. \quad (3)$$

From these equations we find

$$\begin{aligned}\sin\theta/\sin\phi&=N_{AB}|\mathbf{M}_A||\mathbf{M}_B|/N_{AB}'|\mathbf{M}_A||\mathbf{M}_B'|\\&=(N_{AB}/N_{AB}')(1.8/0.2)=9N_{AB}/N_{AB}'.\end{aligned} \quad (4)$$

This is the case because $M_A=g\mu_B S_z N$, $M_B=1.8\,g\mu_B S_z N$, and $M_B'=0.2\;g\mu_B S_z N$, where g is the gyromagnetic ratio, μ_B is the Bohr magneton, S_z is the z component of the spin, and N is the number of formula units per mole.

On rewriting Eq. (2) and by using Eq. (4) we get

$$\cos\theta\simeq 9(N_{AB}/1.8N_{BB}-N_{AB}/N_{AB}')\quad \text{taking } \cos\phi\approx 1. \quad (5)$$

From Fig. 6, on taking the total magnetic moment to be $4.5\mu_B$ and $\cos\phi\simeq 1$, we get $\cos\theta\simeq 0.5$ which requires that

$$0.1=N_{AB}/N_{BB}-1.8N_{AB}/N_{AB}'.$$

Although we do not know N_{AB}'/N_{AB}, i.e., the ratio of the Mn(A)-Mn(B) superexchange interaction to the Mn(A)-Fe(B) superexchange interaction, a reasonable range of values would be from 0.2 to 0.5. In this range, then, we would get $N_{BB}/N_{AB}\approx 0.1$–0.27, which is perhaps not unreasonable for the ratio of the Mn(B)-Fe(B) superexchange interaction to the Mn(A)-Fe(B) interaction. The above discussion shows that the previously assumed spin arrangement can be justified, although whether or not this is the case depends largely on the various superexchange interactions.

This kind of a spin arrangement does not explain the low magnetic moment ($4.6\mu_B$) of the A-site ions as found by Hastings and Corliss.[21] This value may, however, be due to covalency effects which can reduce the value measured by neutron diffraction by a considerable amount.[30]

In Fig. 7(a) we show line 1 of the spectrum obtained in a field of 17 kOe and at room temperature. Also shown is the computer fit to this spectrum comprising the sum of five Lorentzians. The solid line drawn through the data points is the envelope from the fit. The fit was done in a similar way to that for $\mathrm{CoFe_2O_4}$. That is, the intensities of the four Lorentzians composing the B-site line were constrained to be proportional to the probability that an Fe B-site ion has 3, 4, 5, or 6 nearest-neighbor Mn A-site ions. These probabilities have been calculated from Eq. (1) for $c=0.20$. As can be seen from Fig. 7(a), the fit is very good, which means that the model proposed (i.e., that the B-site hyperfine fields depend on the kind of A-site nearest-neighbor ions) describes in detail the Mössbauer spectra. Line 6 of the spectrum shows the same features as line 1. In Table II are listed the hyperfine fields and isomer shifts for the various lines. It is seen that as $6-n$ increases, which means an increase in the number of Mn nearest neighbors, the hyperfine field decreases, whereas the isomer shift remains constant to within the experimental error.

In Figs. 7(b) and 7(c), line 1 of the Mössbauer spectrum is shown together with the computer fit at

TABLE II. Mössbauer data on $\mathrm{MnFe_2O_4}$.

	A	$B1$	$B2$	$B3$	$B4$
H_{hpf} (kOe)	483	461	448	428	413
Isomer shift[a] (mm/sec)	0.43	0.51	0.57	0.52	0.51

[a] Relative to $\mathrm{Fe^{57}}$ in Cr matrix; error in $H_{\mathrm{hpf}}=\pm 5$ kOe, error in IS $=\pm 0.04$ mm/sec.

---

[30] R. Nathans, G. Will, and D. E. Cox, in *Proceedings of the International Conference on Magnetism, Nottingham, 1964* (Institute of Physics and The Physical Society, London, 1965), p. 327.

298 and 475°K. Again line 6 behaves in much the same way. From these spectra it is seen that the separation of the peak positions of the components of the *B*-site line increases as the temperature increases. This indicates that the Mn(*A*)-Fe(*B*) superexchange interaction is less than the Fe(*A*)-Fe(*B*) interaction. It should be pointed out that the *B*-site linewidths are wider than those of the *A* site and increase with

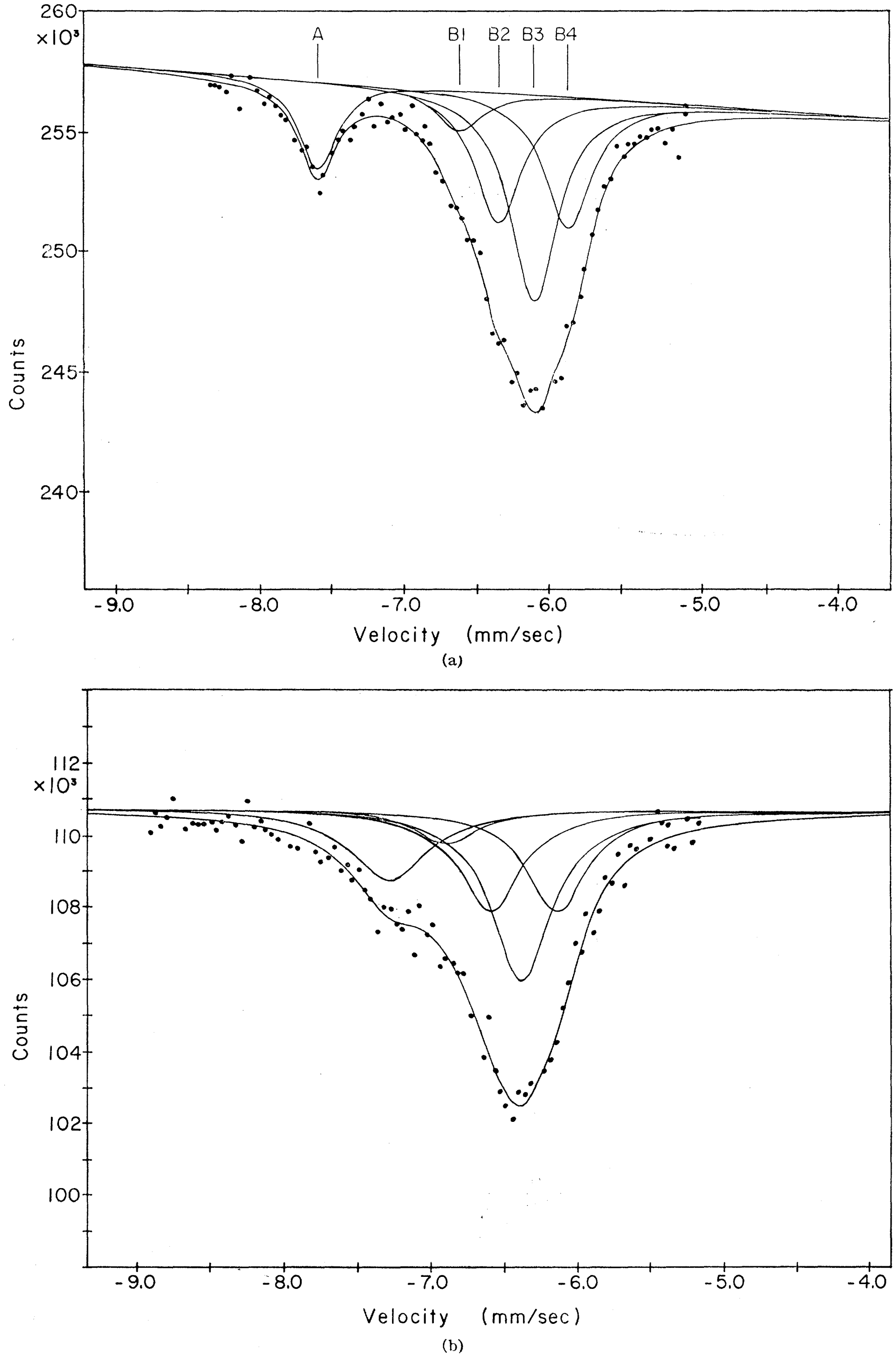

Fig. 7. Line 1 of the Mössbauer spectrum of $MnFe_2O_4$ (a) at 298°K in an applied field of 17 KOe, (b) at 298°K without an applied field, and (c) at 475°K without an applied field. *A* refers to Fe^{57} in *A* sites. *B*: 1, 2, 3, 4 refer to Fe^{57} in *B* sites with 3, 4, 5, 6 nearest-neighbor Mn *A*-site ions, respectively. The Lorentzians shown are those obtained from a least-squares fit to the spectrum. Also shown is the sum of the separate Lorentzians. Line 1 shown in (c) has been corrected for overlap with line 2 of the spectrum.

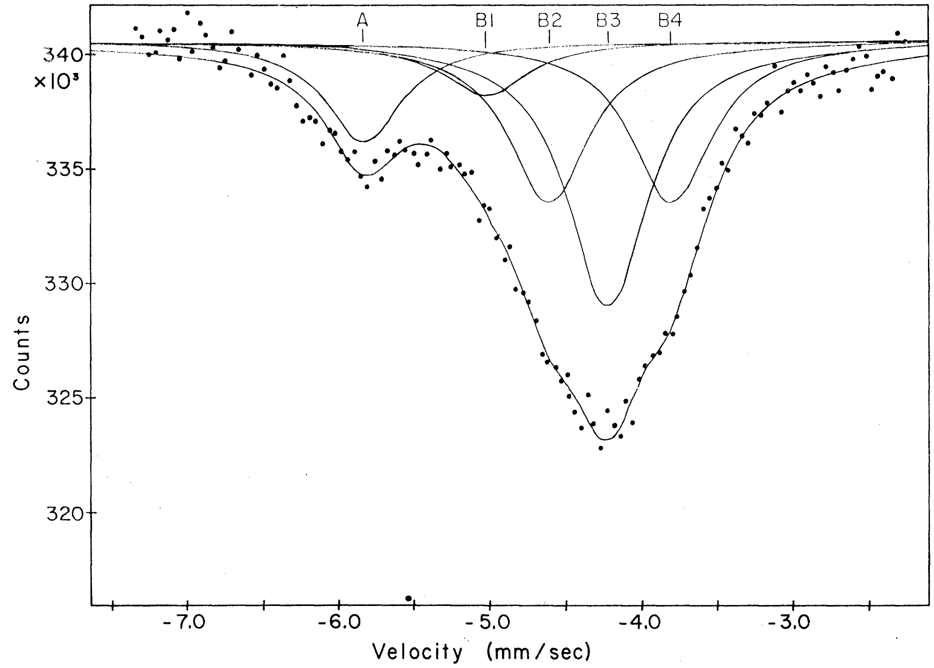

(c)

FIG. 7 (*Continued*)

increasing temperature. This is probably due to next-nearest-neighbor effects which have not been considered in the analysis.

In Fig. 8 is shown the temperature dependence of the various hyperfine fields. The ferrimagnetic Néel temperature was determined to be 573°K by the thermal scanning technique. The distribution in the hyperfine fields at 96 and 7°K was determined from the width of the *B*-site line. Although these values are not very accurate, they indicate that there is a decrease in the *B*-site hyperfine field of about 6 kOe at 0°K when an Fe ion in a nearest-neighbor *A* site is replaced by an Mn ion.

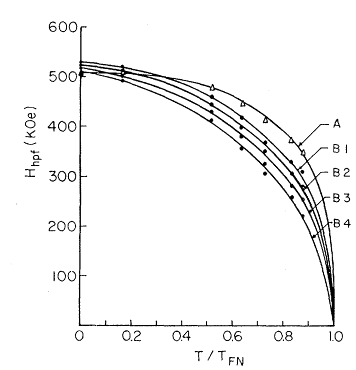

FIG. 8. Temperature dependence of the hyperfine fields at Fe^{57} nuclei in *A* and *B* sites for $MnFe_2O_4$. *B*1, *B*2, *B*3, and *B*4 refer to Fe^{57} *B*-site nuclei with 3, 4, 5, and 6 Mn ions in the nearest-neighbor *A* sites, respectively.

D. $MgFe_2O_4$

A study of the kind just described for $CoFe_2O_4$ and $MnFe_2O_4$ was also carried out for $MgFe_2O_4$. This material is particularly suitable for this kind of study because Mg^{2+} has no net magnetic moment and the degree of inversion of $MgFe_2O_4$ is dependent on the heat treatment.

Mössbauer spectra for $MgFe_2O_4$ (q) and $MgFe_2O_4$ (s.c.) in an applied field of 45 kOe are shown in Figs. 9(a) and 9(b). The area ratio of the absorption lines corresponding to Fe^{57} in *A* and *B* sites was found to be 0.60±0.06 and 0.79±0.06, yielding cation distributions for $MgFe_2O_4$ (q) and $MgFe_2O_4$ (s.c.) given by

$$(Mg_{0.25\pm0.04}Fe_{0.75\pm0.04})[Mg_{0.75\pm0.04}Fe_{1.25\pm0.04}]O_4$$

and

$$(Mg_{0.12\pm0.04}Fe_{0.88\pm0.04})[Mg_{0.88\pm0.04}Fe_{0.12\pm0.04}]O_4,$$

respectively.

The magnetic moments of these materials measured at 4.2°K are $(2.38\pm0.05)\mu_B$ and $(0.82\pm0.02)\mu_B$ per unit chemical formula. The cation distributions calculated from the magnetic moments taking a magnetic moment of $5\mu_B$ per Fe^{3+} ion are in agreement with those measured by the ME.

The Mössbauer spectra shown in Fig. 9 again as for $CoFe_2O_4$ and $MnFe_2O_4$ show broad octahedral lines. The octahedral lines for the $MgFe_2O_4$ (q) are similar in shape to those of $CoFe_2O_4$ (q). The distribution in the *B*-site hyperfine fields can again be explained as

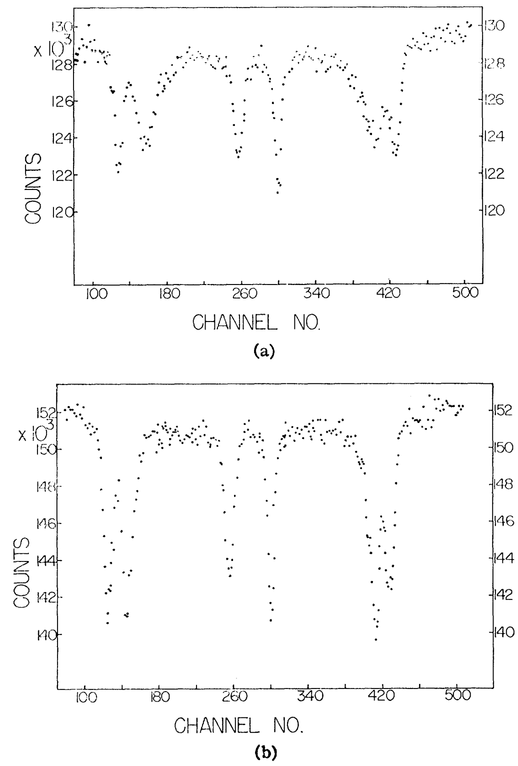

(a)

(b)

FIG. 9. Mössbauer spectra of (a) $MgFe_2O_4$ (q) and (b) $MgFe_2O_4$ (s.c.) in an applied field of 45 KOe at room temperature.

being due to the various possible distributions of Mg and Fe ions in the A sites. Since the Mg ions have no magnetic moment, the Fe-Mg, A-B superexchange interaction will be zero. From this we would expect the octahedral lines to be even broader than for $CoFe_2O_4$ at elevated temperatures. We have collected a number of spectra in the temperature range from 77°K to the ferrimagnetic Néel temperature for both $MgFe_2O_4$ (s.c.) and $MgFe_2O_4$ (q). It is, however, difficult to analyze these spectra because of the large amount of overlap of the A- and B-site lines and also because the A-site lines seem to broaden somewhat at temperatures above 300°K. A detailed analysis has therefore not been done. Qualitatively, however, the spectra can be explained in the same way as was done for $CoFe_2O_4$ and $MnFe_2O_4$. The ferrimagnetic Néel temperatures found by thermal scanning are 612°K for $MgFe_2O_4$ (q) and 679°K for $MgFe_2O_4$ (s.c.).

V. SUPEREXCHANGE INTERACTIONS

In $CoFe_2O_4$, $MnFe_2O_4$, and $MgFe_2O_4$ we found that the temperature dependence of the hyperfine field at Fe^{57} nuclei in B sites and thus the magnetization depends on the number of Co, Mn, Mg, or Fe nearest A-site neighbors of a B-site ion. With the use of molecular-field theory we can calculate from the experimental data the Fe(A)-Fe(B), Co(A)-Fe(B) and Mn(A)-Fe(B) superexchange interactions. Although the molecular theory does not give a correct relation between the transition temperature and the exchange interaction for both ferro- and antiferromagnets, we should, however, be able to get reasonable values for the ratio of the Co(A)-Fe(B) and Mn(A)-Fe(B) superexchange interactions to the Fe(A)-Fe(B) interactions.

In the molecular-field approximation, the molecular field acting on a B-site ion can be written as

$$\mathbf{H}(B)=\sum_i N_{A_iB}\mathbf{M}_{A_i}+\sum_j N_{B_jB}\mathbf{M}_{B_j}, \quad (6)$$

where N_{A_iB} and N_{B_jB} are the molecular-field coefficients corresponding to A-B and B-B superexchange interactions. The sum is taken over all different kinds of ions in the two sites. Since we are measuring only the temperature dependence of the magnetization for the Fe^{3+} ions we will be concerned with calculating N_{A_iB} where B will refer to an Fe^{3+} ion. If the molecular fields are due to nearest-neighbor interactions only we can write Eq. (6) in terms of the exchange integrals J. Thus we have

$$H(B)=2J_1n\langle S_z(A_1)\rangle+2J_2(6-n)\langle S_z(A_2)\rangle, \quad (7)$$

where we have neglected B-B interactions and have assumed that there are only two kinds of ions in the A sites. J_1 and J_2 are then the exchange integrals corresponding to the two types of A-site ions, n is the number of nearest-neighbor A-site ions of type 1, and $(6-n)$ is the number of nearest-neighbor A-site ions of type 2. $\langle S_z(A)\rangle$ is the average value of the z component of the spin for the two types of ions referred to with subscripts 1 and 2. From Eq. (7) we see that, if $J_1\neq J_2$, then the molecular field will depend on n and S_z.

The temperature dependence of the magnetic moment of an Fe ion with n nearest neighbors of type 1 and $(6-n)$ of type 2 will be given by

$$\langle S_z(\mathrm{Fe}(B))\rangle_n=\tfrac{5}{2}B_{5/2}[2J_1n\tfrac{5}{2}\langle S_z(A_1)\rangle+2J_2(6-n)\tfrac{5}{2}\langle S_z(A_2)\rangle]/kT, \quad (8)$$

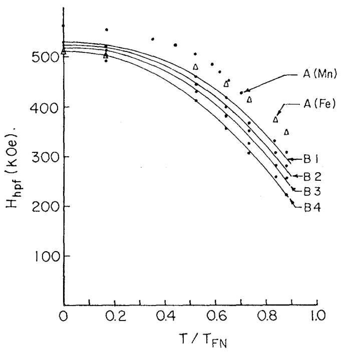

FIG. 10. Temperature dependence of the hyperfine fields for $MnFe_2O_4$. B:1, 2, 3, 4 refer to Fe^{57} in B sites with 3, 4, 5, 6 Mn A-site nearest neighbors, respectively. The curves shown are calculated theoretically as described in the text.

Where $B_{5/2}$ is the Brillouin function for spin $\frac{5}{2}$. In Fig. 10 we show again the various magnetization curves as found for $MnFe_2O_4$. Also shown is the Mn(A) magnetization curve as measured by Yasuoka *et al.*[31] using NMR techniques. The solid lines drawn are the theoretical curves calculated using Eq. (8). For $\langle S_z(A_1)\rangle$ we chose the values we measured for Fe in A sites and for $\langle S_z(A_2)\rangle$ we chose the values determined by Yasuoka *et al.*[31] for Mn in A sites. The parameters J_1 and J_2 were then varied until the best fit was obtained. The values for the curves drawn in Fig. 10 are $J_1=18.4$°K and $J_2=12.1$°K. The ratio of the Mn(A)-Fe(B) to Fe(A)-Fe(B) superexchange interaction is then $J_2/J_1=0.66\pm0.04$.

In Fig. 11 we reproduce the $CoFe_2O_4$ data together with the theoretical calculated curves. Since we did not have any information about the Co A-site magnetization curve, we used for this the same values as for the Fe A-site magnetization—however, with a spin $\frac{3}{2}$ for the Co ion. The values of J_1 and J_2 were found to be 20.07 and 13.7°K, respectively. The ratio of the Co(A)-Fe(B) to Fe(A)-Fe(B) superexchange interaction is then 0.68 ± 0.04. It should be noted that the value for J_1 determined for $CoFe_2O_4$ is close to that determined from the $MnFe_2O_4$ data. The Fe-Fe superexchange interaction calculated from T_{FN} for Li ferrite is $J=22$°K. A decrease in J is expected in going from Li to Co to Mn ferrite because of an increase in lattice parameters. Indeed, the lattice parameters increase from 8.33 to 8.38 to 8.51 Å, respectively. This shows that the values found for the Fe-Fe superexchange interaction are in qualitative agreement with the Fe-O distances in the materials considered.

That the A-site magnetization curve for Fe^{3+} ions seems to be quite independent of the kind of B-site nearest neighbor is evident from the relatively narrow lines found in the Mössbauer spectra for $NiFe_2O_4$, $CoFe_2O_4$, and $MnFe_2O_4$. An A-site iron ion is surrounded by 12 nearest B neighbors. In an inverse spinel there are, on the average, six iron ions among these. By making the spinel less inverse, the effects go in opposite directions for the A- and B-site ions. An A-site ion is getting more nearest iron B neighbors, while the average number of nearest iron A neighbors for a B site decreases. On assuming that the $Fe^{3+}(B)$-$Fe^{3+}(A)$ superexchange strength is the strongest, the total superexchange strength felt by a $Fe^{3+}(A)$ ion increases as the degree of inversion decreases. Only narrowing of lines might be expected in the spectra of $CoFe_2O_4$, $MgFe_2O_4$, and $MnFe_2O_4$. However, since the lines in $NiFe_2O_4$ are already relatively narrow, this effect may be quite small.

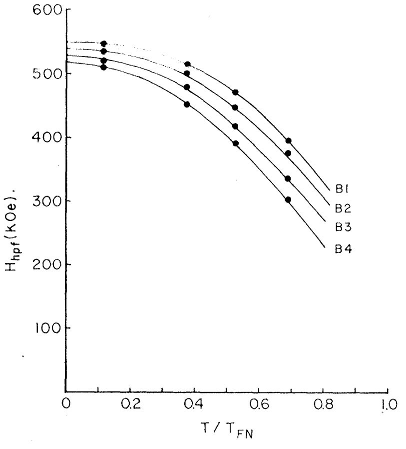

FIG. 11. Temperature dependence of the hyperfine fields for $CoFe_2O_4$ (q). B:1, 2, 3, 4 refer to Fe^{57} in B sites with 0, 1, 2, 3 Co A-site nearest neighbors, respectively. The curves shown are calculated as described in the text.

VI. CONCLUSION

With M = Ni, Co, Mn, or Mg, the results on the ferrimagnetic spinels $(Fe_{1-x}M_x)[Fe_{1+x}M_{1-x}]O_4$ show that the broadened Mössbauer spectra for not completely inverse spinels $(1>x>0)$ are physically meaningful. For $x=0$, as for $NiFe_2O_4$ each Fe^{3+} B-site ion is surrounded by six A-site Fe^{3+} ions. The lines ascribed to B-site ions have approximately the same width as those attributed to A-site ions and are relatively narrow. For $MgFe_2O_4$, x depends on the heat treatment, and broadened B lines are observed. With $x\neq0$, B-site ions have Mg(A) neighbors not possessing a magnetic-dipole moment. Hence the total superexchange strength of a central Fe^{3+} (B) ion is reduced, and so also is the expectation value of the magnetic moment at higher temperatures, which explains the broadened Mössbauer lines. In $CoFe_2O_4$ and $MnFe_2O_4$ with $x\neq0$, line broadening in the Mössbauer spectra was observed also because the $Fe^{3+}(B)$-$Co^{2+}(A)$ and $Fe^{3+}(B)$-$Mn^{2+}(A)$ superexchange is weaker than the $Fe^{3+}(B)$-$Fe^{3+}(A)$ superexchange. In all these cases the degree of broadening could be related to the number of most probable distributions in the nearest A-site neighbors. From the shape of the H_{hpf} versus T curves, the relation $Fe^{3+}(B)$-$Co^{2+}(A)$ and $Fe^{3+}(B)$-$Mn^{2+}(A)$ superexchange strength has been determined to be 0.68 and 0.66, respectively, of the $Fe^{3+}(B)$-$Fe^{3+}(A)$ superexchange strength.

The various explanations for the low magnetic moment per unit chemical formula in $MnFe_2O_4$ have been tested. No Fe^{2+} ions have been observed, and also evidence for canting of the $Fe^{3+}(B)$ moments could not be found. A model in which the $Mn^{2+}(B)$ moments are assumed to be canted is discussed and shown to be consistent with most of the results.

---

[31] H. Yasuoka, J. Phys. Soc. Japan **19**, 182 (1964).